

Supporting information - Atomistic modeling of site exchange defects in lithium iron phosphate and iron phosphate

Christian Kuss¹, Guoxian Liang², Steen B. Schougaard^{1,*}

1 Department for Chemistry, Université du Québec à Montréal, 2101 rue Jeanne-Mance, Montreal (QC) H1X 2J6, Canada

2 Phostech Lithium Inc., 1475 rue Marie-Victorin, St.Bruno de Montarville (QC) J3V 6B7, Canada

Table S1. Mechanical properties, dielectric constants and heat capacities of LiFePO₄ and FePO₄ from atomistic calculations.

	LiFePO ₄	FePO ₄
Bulk moduli		
K _{Reuss}	117.3 GPa	63.9 GPa
K _{Voigt}	118.0 GPa	64.4 GPa
K _{Hill}	117.6 GPa	64.1 GPa
Shear moduli		
G _{Reuss}	56.8 GPa	36.9 GPa
G _{Voigt}	59.6 GPa	42.5 GPa
G _{Hill}	58.2 GPa	39.7 GPa
Youngs moduli		
E _a	142.9 GPa	111.0 GPa
E _b	179.6 GPa	179.5 GPa
E _c	151.0 GPa	97.2 GPa
Dielectric constants		
ε ₀	19.8	17.5
ε _{hf}	3.77	5.19
Heat capacities		
C _p , 100K	43.5 J/(K.mol)	35.1 J/(K.mol)
C _p , 200K	87.8 J/(K.mol)	70.3 J/(K.mol)
C _p , 300K	113.6 J/(K.mol)	92.5 J/(K.mol)
C _p , 400K	129.7 J/(K.mol)	107.1 J/(K.mol)
C _p , 500K	140.2 J/(K.mol)	116.8 J/(K.mol)
C _p , 600K	147.1 J/(K.mol)	123.3 J/(K.mol)

To assess the transferability of the set of potentials, we calculated the optimized crystal structures of γ-Li₃PO₄ and the Nasicon analogue Li₃Fe₂(PO₄)₃:

Table S2. Comparison of calculated and experimental crystal structure parameters of γ-Li₃PO₄.

Li ₃ PO ₄	Experimental ¹	Calculated	Rel. error / %
a / Å	6.12	6.03	1.5
b / Å	10.53	10.27	2.5
c / Å	4.93	4.87	1.2
Li ₃ Fe ₂ (PO ₄) ₃	Experimental ²	Calculated	Rel. error / %
a / Å	8.32	8.20	1.4
c / Å	22.46	21.63	3.7

It can be seen, that the potentials are valid with restrictions also for other compounds of the lithium and iron phosphate system. Note: This potential set should only be used for structures where oxygen is covalently bonded to phosphor in phosphate groups.

For calculations of defect correlation, we determined a quantity of charge localization on the unit cell scale. This quantity was determined from the relaxed structures by integrating all charges within the volume of one unit cell. This volume was then moved across the complete super cell by $\frac{1}{4}$ unit cell steps in each crystallographic direction to obtain an average of charge localization in the super cell.

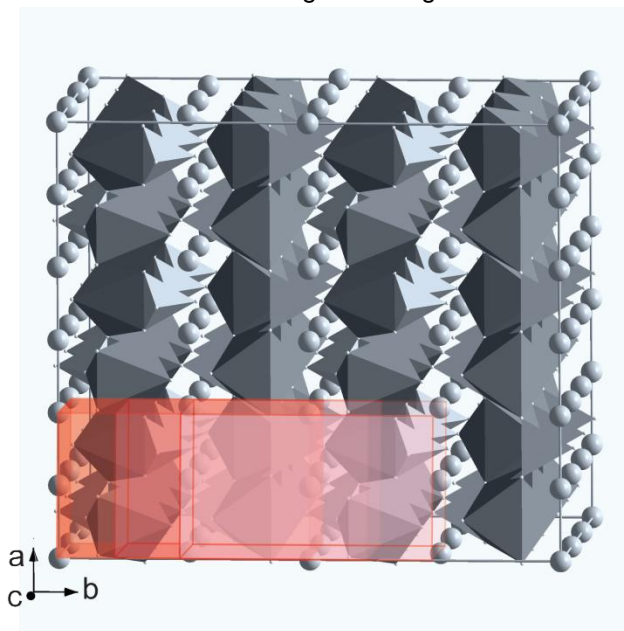


Figure S1. Illustration of iterative charge integration to obtain the value termed average localized charge.

The red cuboids correspond to the volume of one unit cell each. The left cuboid determines the integration boundaries for the first integration step. The other cuboids illustrate the movement of the integration boundaries during the iterative integration over the whole super cell. An average of integrated charge per unit cell is then determined for the complete super cell.

References

1. J. Zemmann, *Acta Crystallographica*, 1960, **13**, 863-867.
2. C. Masquelier, C. Wurm, J. Rodríguez-Carvajal, J. Gaubicher and L. Nazar, *Chem. Mater.*, 2000, **12**, 525-532.